GaNAs as Strain Compensating Layer for 1.55 μm Light Emission from InAs Quantum Dots

To cite this article: Sasikala Ganapathy *et al* 2003 *Jpn. J. Appl. Phys.* **42** 5598

Jpn. J. Appl. Phys. Vol. 42 (2003) pp. 5598–5601
Part 1, No. 9A, September 2003

GaNAs as Strain Compensating Layer for 1.55 μm Light Emission from InAs Quantum Dots

Sasikala GANAPATHY[1,2*], Xi Qing ZHANG[1], Ikuo SUEMUNE[1,2], Katsuhiro UESUGI[1], Hidekazu KUMANO[1], B. J. KIM[3] and Tae-Yeon SEONG[3]

[1]*Research Institute for Electronic Science, Hokkaido University, Kita-12, Nishi-6, Sapporo 060-0812, Japan*
[2]*CREST, Japan Science and Technology Corporation, 4-1-8, Honcho, Kawaguchi,332-0012 Japan*
[3]*Centre for Frontier Materials and Department of Material Science and Engineering, Kwangju Institute of Science and Technology, Kwangju 500-712, Korea*

(Received March 4, 2003; accepted for publication March 28, 2003)

GaNAs strain-compensating layers (SCLs) are applied to bury InAs quantum dots (QDs) grown on GaAs substrates. The main idea is the compensation of the compressive strain induced by InAs QDs with the tensile strain in the GaNAs SCLs to keep the total strain of the system minimum. The application of the GaNAs SCLs resulted in a systematic shift of photoluminescence (PL) peaks of the InAs QDs toward the longer wavelengths with the increase of the nitrogen (N) composition in GaNAs, and luminescence at a wavelength of 1.55 μm has been achieved from the InAs QDs for the N composition of 2.7% in the GaNAs SCL. This result is promising for the application of GaNAs SCL for InAs-QDs-based long-wavelength light sources for optical-fiber communication systems. [DOI: 10.1143/JJAP.42.5598]

KEYWORDS: GaNAs, strain compensating layer (SCL), InAs quantum dot, photoluminescence, long-wavelength

1. Introduction

Self-assembled InAs quantum dots (QDs) have been studied extensively.[1–4] In addition to intrinsic features specific to QDs, one of the most attractive capabilities will be the extension of the emission wavelength of InAs QDs grown on GaAs to 1.3 and 1.55 μm.[1–8] The crucial point has been attributed to the residual strain inside QDs, and many efforts have been devoted towards the strain compensation of InAs QDs to obtain the longer-wavelength emission.[2–7] InAs QDs in general experience strain due to the following two reasons: 1) Compressive strain induced inside the dots due to the lattice mismatch between InAs and GaAs substrate, which is the driving force for the Stranski–Krastanow (S–K) growth of InAs QDs. 2) Additional compressive strain is introduced into the dots from a matrix when they are buried.[6]

In the case of non-buried InAs QDs, compressive strains induced inside the dots were relieved towards the dot surfaces since they are under the stress-free condition. Therefore, the uncapped InAs QD grown on a GaAs substrate illustrated in Fig. 1(a) will experience lower compressive strain than the buried one. Emission from such open dots shows red shift to the longer wavelength due to the reduced strain effect on the energy gap.[6] On the other hand, when the dots are buried inside a GaAs or InGaAs matrix for device applications as illustrated in Fig. 1(b), the emission from the InAs QD will be blue-shifted towards the shorter wavelength due to the compressive-strain-induced increase of the energy gap in the dots.[6]

When InAs QDs are embedded in a GaAs or InGaAs matrix, the net compressive strain originating from the InAs QDs remains in the system and will be accumulated with the increase of the stacks of InAs QDs layers. In some applications of InAs QDs such as detectors[9] or quantum logic gates,[10] multi-stacking of the InAs QDs are essentially important. Semiconductor laser diodes based on QDs tend to face gain saturation due to the finite volume of QD arrays. Multi-stacking of the QDs layers is also an effective method to overcome this gain saturation issue of QD lasers.[11] The accumulation of the net compressive strain with the multi-stacking of InAs QDs in the system will result in the higher probability of plastic relaxations along the growth direction,[12] which will reduce the device reliability in the relevant applications.

Based on these considerations, InAs QDs embedded in GaNAs strain-compensating layers (SCLs) are proposed in this letter. The residual tensile strain in the GaNAs capping layer will compensate the net compressive strain induced by the InAs QDs as shown in Fig. 1(c). The strain compensation issue will be discussed with transmission electron microscopy (TEM) measurements. The optical properties of the

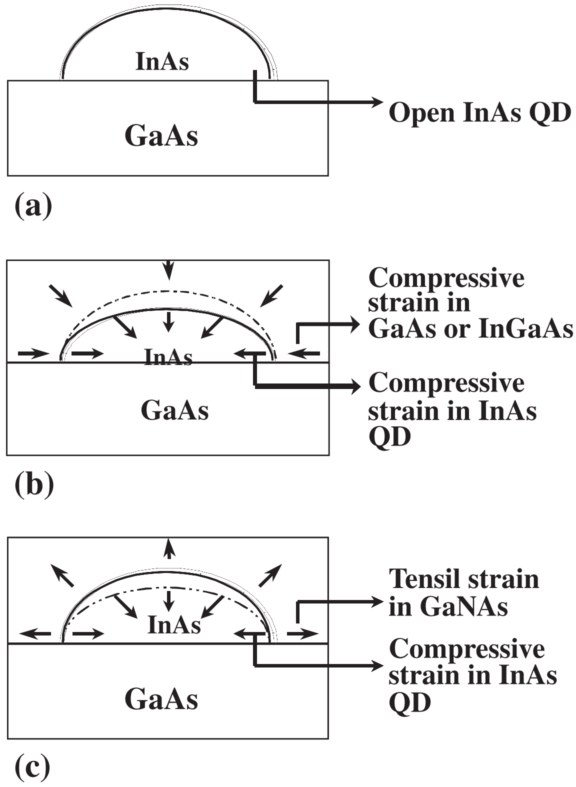

Fig. 1. (a) Schematics of surface quantum dots with strain relaxation, (b) quantum dots burried in the strain reducing InGaAs layer and (c) quantum dots burried in the strain componsating GaNAs layer.

*Corresponding author. E-mail address: sasikala@es.hokudai.ac.jp

InAs QDs are studied and the improvement of the photo luminescence properties with the application of the GaNAs SCLs will be discussed. It is also demonstrated that the PL emission wavelength from the InAs QDs are monotonically red-shifted with the increase of the nitrogen (N) composition in the GaNAs SCLs, and the observation of PL emission around the wavelength of 1.55 μm will be demonstrated.

Samples were grown on semi-insulating GaAs (001) substrates by metalorganic-molecular-beam epitaxy (MOMBE). The metalorganic precursors used were triethylgallium (TEGa), triethylindium (TEIn), trisdimethylaminoarsenic (TDMAAs), and monomethylhydrazine (MMHy) with the respective beam equivalent pressure (BEP) of 8×10^{-4} Pa, 0.8×10^{-4} Pa, 30×10^{-4} Pa, and $50–200 \times 10^{-4}$ Pa. The growth procedure was as follows. After oxide desorption from a GaAs substrate surface, a 100-nm-thick GaAs buffer layer was grown at 550°C. The substrate temperature was then lowered to 400°C, and about 2.0 monolayers (ML) of InAs were deposited with a pulsed supply of TEIn at a medium growth rate of 0.1 ML/s. TDMAAs was continuously supplied during the growth of InAs. A transition from two-dimensional to three-dimensional growth mode, i.e., the initiation of the Stranski–Krastanow growth mode, was confirmed with the reflection high-energy electron diffraction (RHEED) by the pattern transform from streaks to chevrons. After the growth of the first stack of InAs QDs, ~10-nm-thick GaNAs SCL was grown with different nitrogen compositions (0–2.7%) and then ~10-nm-thick GaAs buffer layer was grown for the growth of the next stack at the same substrate temperature. Similar growth conditions were used for the growth of the second stack of the layers. The N composition in the GaNAs layers was estimated with symmetric (004) and asymmetric (224) high-resolution X-ray diffraction measurements to estimate the elastic distortion of the layers and with the assumption of the Vegard's law between the lattice constants of the constituent binary compounds. The local lattice distortion around the InAs QDs due to the strain field is examined by cross-sectional TEM observations. The PL measurements were carried out using the second harmonic generation of a YAG laser at the wavelength of 532 nm. The measurements were performed between 18 K and room temperature in a closed-cycle "He" cryostat. A liquid-nitrogen-cooled germanium detector was used to measure the signal dispersed by a 0.5-m monochromator via lock-in mode detection scheme.

Figures 2(a), 2(b) and 2(c) show cross-sectional TEM images of InAs QDs. The surface density of the dots examined with atomic force microscopy (AFM) was $\sim 1 \times 10^{11}$ dots/cm^2 and the lateral intervals of the QDs observed in Figs. 2(a) and 2(b) are almost consistent with the AFM observation of the open structures. The average dot height is 3 nm and the average dot base diameter is 25 nm. The dots shown in Figs. 2(a), 2(b), and 2(c) are buried inside the 10 nm-thick GaNAs SCLs with N = 0.5%, 0.7%, and 2.7%, respectively. Figures 2(a) and 2(b) have two-stacks of QD layers, whereas Fig. 2(c) has one stack.

Concerning the TEM observations, the stain effects will be discussed from the following three points: (1) fringe due to lattice distortions induced by the strain around InAs QDs, (2) comparison of the dot size in the two stacks of InAs QDs layers, (3) strain-induced alignment of the dots in the two stacks of the layers. In the sample grown with the lower N composition of 0.5% in the GaNAs SCL [Fig. 2(a)], the strain fields around the dots are present from the following findings: (1) Very clear fringe induced by the lattice distortion is present around the dots. (2) The dots in the upper layer are slightly bigger than those in the lower layer. This is usually observed by the penetrated strain field, which will change the initial growth condition of the InAs QDs in the upper stack of the layer. (3) The dots are vertically aligned with the strain field penetrating into the adjacent layer.[12]

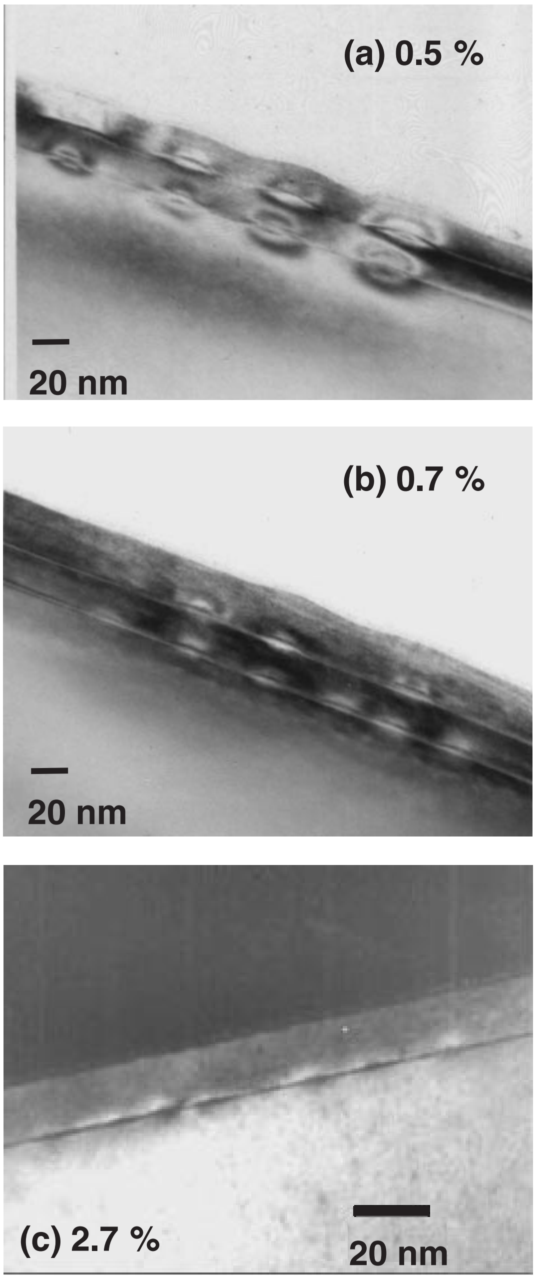

Fig. 2. Cross-section TEM images of the two stacked InAs QDs buried in the GaNAs SCL (a) N: 0.5%, (b) N: 0.7% and single stacked (c) N: 2.7%.

On the other hand, in the sample grown with the higher nitrogen composition of 0.7% [Fig. 2(b)], the strain fields around the dots are substantially reduced, which is evidenced by the following: (1) the lattice distortion around the InAs QDs is much reduced. (2) The dot size in the two stacks is similar. (3) The dots formed in the upper layer are partially aligned to the dots underneath, and some of the dots are missing in the upper stack. These demonstrate the strain compensation effect with the GaNAs SCLs. Unfortunately the sample for the GaNAs SCL with N = 2.7% shown in Fig. 2(c) has only one stack, but it will be clear that the strain field around the QDs is further reduced in comparison to the others samples shown in Figs. 2(a) and 2(b). Although the crystalline quality is usually degraded in GaNAs with the higher N composition, it will be seen that there is no apparent additional defects observed with this high N composition of 2.7%.

To investigate the strain compensation effect of the SCL further, the dependence of PL spectra and PL intensities on the selection of the capping layer for InAs QDs was examined with the constant photo-excitation intensity of 9.5 W/cm^2 and at 20 K. Figure 3 shows the PL spectra measured from InAs QDs capped with GaNAs SCLs with different N compositions of 0%, 0.5%, and 0.7%. Two peaks of '*s*' (ground state) and '*p*' (first exited state) were observed in the PL spectrum from the InAs QDs capped with the GaAs spacer layers. When InAs QDs were capped with the GaNAs SCLs with 0.5% nitrogen, '*p*' state became more prominent and '*d*' state (second exited state) emerged. When the N mole fraction in the SCL was increased further to 0.7%, '*f*' (third exited state) and '*g*' (fourth exited state) started appearing. These results indicate that the increase of the N composition in the SCL enhances the state filling effect, i.e. the shells of the QDs are progressively populated with the photoexited carriers under the constant excitation densities. These results indicate that nonradiative recombinations are progressively reduced with the GaNAs SCLs with the higher N compositions, which will be attributed to the reduced defect densities with the net strain compensation with the tensile-strained SCLs.

There have been several reports on the observation of well-defined QD shells, but most of them are with the lower dot density of $\sim 10^9$–10^{10} dots/cm^2.[4,13)] It is noted that the present InAs QDs have the much higher surface density of $\sim 1 \times 10^{11}$/cm^2 and the PL spectra were measured from the two stacks of InAs QDs layers. Under the similar conditions, the shell states have been rarely observed before. Therefore the observation of the well-defined shell states in the present study will be attributed to the improved homogeneity of the InAs QDs with the net stain compensation with the GaNAs SCLs.

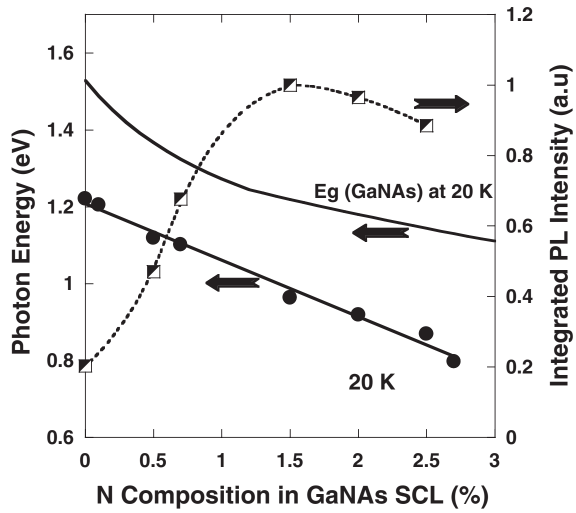

Fig. 4. The PL peak wavelength and integrated PL intensity dependence on the N composition in the GaNAs SCL with GaNAs reference. While most of the samples have two stacks of InAs QDs layers, the sample with the N composition of 2.7% has one stack.

Figure 4 shows the N composition dependence of the PL peak emission wavelength of the ground state. It is shown that the increase of the N composition in the GaNAs SCLs induces the red shift of the PL peak wavelength toward the longer wavelength. Furthermore, it can be seen from Fig. 4 that the PL integrated intensity observed from the InAs QDs is increased with the increase of the N composition in the GaNAs SCLs up to 1.5% and above this the intensity starts to decrease. These results indicate that the optical quality of the InAs QDs buried in the GaNAs SCLs is much improved with the concept of the net strain compensation.

The above measurements suggested that 1.55 μm emission from InAs QDs would be possible with the GaNAs SCLs, which have the N composition of 2.7%. Figure 5 shows a PL emission spectrum measured at room temperature from the InAs QDs buried in the GaNAs SCL with the nitrogen composition of 2.7%. The additional peak appeared at the wavelength of 1009 nm will correspond to the InAs wetting layer.

The precise description of the red-shift observed in Fig. 4 is now under the study. Concerning the diffusion effect at the interface between the InAs QDs and GaNAs SCLs, the present samples were grown at the lower temperature of 400°C to prevent the influence of the interface diffusion. We also examined the diffusivity of Ga, In or N at the interface with post-growth thermal annealing. The PL spectra showed slight blue shift rather than red shift after annealing, and this shows that the diffusivity of Ga into InAs is higher than that of N.

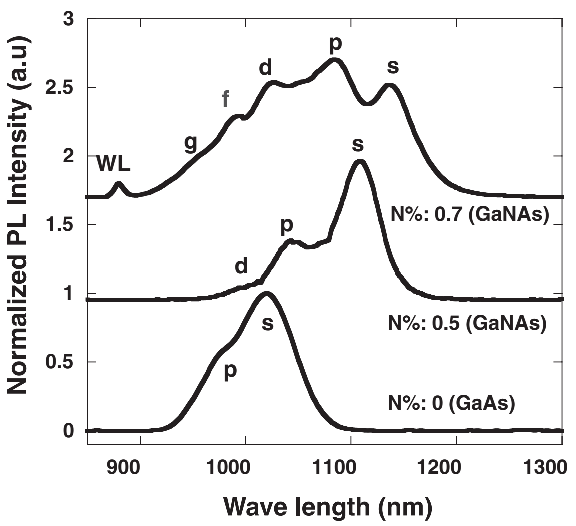

Fig. 3. PL spectrum of the InAs QDs embedded in the GaNAs SCL with different nitrogen compositions at 20 K.

As a reference, the GaNAs energy gap with respect to the nitrogen mole fraction is also plotted in Fig. 4, which shows nice fit to the measured N composition dependence of the GaNAa energy gap.[14)] Since the band offset at the Ga(N)As/

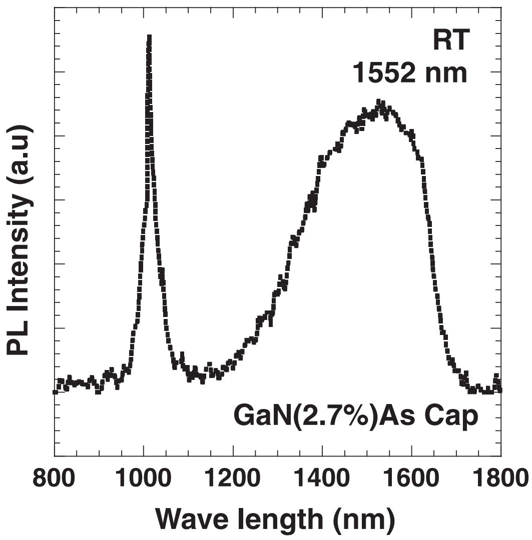

Fig. 5. 1.55 μm light emission from InAs quantum dots buried in $GaN_{0.027}As_{0.973}$ strain-compensating layer at room temperature.

InAs heterointerface is localized in the conduction band,[15,16) the reduction of the energy gap of the GaNAs SCL will mainly reduce the conduction band offset. This will suggest that the dominant contribution to the measured red shift of the luminescence from the InAs QDs for the smaller N composition will be the reduction of the conduction band offset. On the other hand, a theoretical calculation of the strain field with a valence-force field model evidenced the contribution of the GaNAs SCL for reducing the compressive strain field inside the InAs QDs. More detailed quantitative discussions in the whole N composition will be given in future publications.

In summery, the function of the GaNAs SCL in compensating the compressive strain induced by the InAs QDs was demonstrated with the TEM and PL measurements. The systematic red shift of the PL emission wavelength up to ~1.5 μm was demonstrated with the increase of the N composition in the tensile-strained GaNAs SCL. These results show the possibility to realize light emitter with long-wavelength emission over 1.5 μm from the InAs QDs with the application of the GaNAs strain-compensating layers.

The authors are grateful to Mitsuo Hoshiyama for his technical assistance during this work. This work was supported in part by Japanese Society for the promotion of Science (JSPS) programme and one of the authors (S. G.) wishes to express her thanks to JSPS for a JSPS award and Grant-in-aid support. This work was also supported in part by the Telecommunications Advancement Organization of Japan and by the Grant-in-Aid for Scientific Research on Priority Area (A), No. 13026201 from the Ministry of Education, Culture, Sports, Science and Technology.

1) M. Sopanen, H. P. Xin and C. W. Tu: Appl. Phys. Lett. **76** (2000) 994.
2) J. Tatebayashi, M. Nishioka and Y. Arakawa: Appl. Phys. Lett. **78** (2000) 3469.
3) V. M. Ustinov, N. A. Maleev, A. E. Zhukov, A. R. Kovsh, A. Yu. Egorov, A. V. Lunev, B. V. Volovik, I. L. Krwstnikov, Yu. G. Musikhin, N. A. Bert, P. S. Kop'ev, Zh. I. Alferov, N. N. Ledentsov and D. Bimberg: Appl. Phys. Lett. **74** (1999) 2815.
4) D. L. Huffaker, G. Park, Z. Zou, O. B. Shchekin and D. G. Deppe: Appl. Phys. Lett. **73** (1998) 2564.
5) G. Park, O. B. Shchekin, S. Osutak, D. L. Huffaker and D. G. Deppe: Appl. Phys. Lett. **75** (1999) 3267.
6) H. Saito, K. Nishi and S. Sugou: Appl. Phys. Lett. **73** (1998) 2742.
7) K. Nishi, H. Saito, S. Sugou and J.-S. Lee: Appl. Phys. Lett. **74** (1999) 1111.
8) K. Mukai and M. Sugawara: Appl. Phys. Lett. **74** (1999) 3963.
9) H. C. Liu, M. Gao, J. McCaffrey, Z. R. Wasilewski and S. Fafard: Appl. Phys. Lett. **78** (2001) 79.
10) H. Sasakura, S. Muto and T. Ohshima: Physica E **10** (2001) 458.
11) Y. Qiu, P. Gogna, S. Forouhar, A. Stintz and L. F. Lester: Appl. Phys. Lett. **79** (2001) 3570.
12) M. O. Lipinski, H. Schuler, O. G. Schmidt, K. Eberl and N. Y. Jin-Phillipp: Appl. Phys. Lett. **77** (2000) 1789.
13) N. Perret, D. Morris, L. Franchomme-Fosse, R. Cote, S. Fafard, V. Aimez and J. Beauvais: Phys. Rev. B **62** (2000) 5092.
14) I. Suemune, K. Uesugi and W. Walukiewicz: Appl. Phys. Lett. **77** (2000) 3021.
15) S.-H. Wei and A. Zunger: Appl. Phys. Lett. **72** (1998) 2011.
16) C. G. Van De Walle: Phys. Rev. B **39** (1989) 1871.